SAND2009-4392C

Chemical, Phase, and Interface Effects in Solution-Based Fabrication of Ferroelectric Thin Film Capacitors

Geoff L. Brennecka, Chad M. Parish, Jacob Jones*, Bruce A. Tuttle, Jill S. Wheeler, and John G. Ekerdt‡

Sandia National Laboratories, Albuquerque, NM, USA 87185
Fax: 81-505-844-9781, e-mail: glbrenn@sandia.gov
*University of Florida, Gainesville, FL, USA 32611
Fax: 81-352-846-3355, e-mail: jjones@mse.ufl.edu
‡University of Texas at Austin, Austin, TX, USA 78712
Fax: 81-512-471-7060, e-mail: ekerdt@che.utexas.edu

ABSTRACT: Thin film ferroelectrics, generally based on modified $Pb(Zr,Ti)O_3$ or $(Ba,Sr)TiO_3$ compositions, represent a small but important portion of the overall capacitor market, particularly for fully-integrated, low-voltage applications. While solution deposition offers several advantages for the fabrication of these types of devices, it is accompanied by many challenges as well, including precise control of film stoichiometry, cation homogeneity, microstructure development during crystallization, electrode interactions, as well as yield and reliability at the wafer lever. Such issues are of increasing importance as dielectric layer thicknesses shrink below 50nm and as multilayer structures are investigated for maximum areal capacitance density. Reliable and robust use of such ultrathin multilayer capacitors at extremely high operating electric fields requires a fundamental understanding and, ideally, mitigation of potential defect origins at every stage of fabrication. This paper describes recent advances in characterizing and controlling the evolution from liquid solution to ceramic film, with a focus on the role of electrodes in phase and interface development as well as film structure and properties, and the resulting effects on single and multilayer capacitor performance and reliability.

Key words: thin film, interface, $Pb(Zr,Ti)O_3$, solution deposition

1. INTRODUCTION

Researchers have long recognized the critical roles that phase content and distribution play in the properties of ferroelectric materials. Unfortunately, few studies have actually investigated the interfaces in enough detail to provide a comprehensive description of not only the effects of the interfaces on electrical behavior, but also the origins and nature of the interfaces themselves. Too often, a change in measured response is correlated with a change in feature size, and the claim is made that this observation is representative of a broad and general 'size effect'. An excellent example of this is the ever-decreasing value of the famous critical feature size for ferroelectricity. Claimed (and somewhat generally-accepted) values for this critical size were originally discussed in terms of numbers of microns, then nanometers, and now unit cells. There have certainly been individual reports that could serve as counter-examples, but for the most part, the generally accepted values for fundamental size constraints on ferroelectricity have shrunk along with the associated capabilities of fabrication and characterization technologies.

Naturally, our knowledge improves as the capabilities of the investigative tools at our disposal advance, but there is danger in making broad conclusions from narrow studies—in focusing so intently upon a new and/or improved tool that complimentary techniques are overlooked. The purpose of this paper is not to claim a new discovery related to the fundamental size effects of ferroelectric materials, but rather to summarize several years of work on a specific materials system in order to illustrate how much and how little we know about phase and interface development in technologically-relevant materials systems based on ferroelectric thin films, with a specific focus on capacitor applications. The literature is rife with examples of the critical importance of interfaces in electroceramics; we begin with a discussion of some of the best and most representative studies from our colleagues around the world, then concentrate on the phase and interface development of a specific example system, solution-deposited ferroelectric thin films based on the lead zirconate titanate (PZT) system.

2. CRITICAL INTERFACES

Ferroelectricity is a collective phenomenon that arises from the interactions among neighboring permanent (spontaneous) dipoles which ultimately results in a macroscopic net polarization that can be reoriented with the application of an electric field. As first pointed out by Ginzburg, the possibility of reorientable dipoles will disappear when either the surface or screening energy of a system becomes larger than the lattice energy that produces the dipoles.[1] Further, since the definition of ferroelectricity requires actual demonstration of the reorientation of these

dipoles, it is possible for spontaneous dipoles to exist but for other factors to so dominate the electrical behavior of a sample as to preclude its demonstration as a true ferroelectric. Such is the case, for example, in very conductive materials that are unable to sustain sufficient electric field to flip their permanent dipoles.

The stipulation for experimental demonstration of polarization rotation does not mean that the value of theory and modeling is in any way reduced in the ferroelectrics field. On the contrary, as demonstrated in this work and many others, the complexity involved in the materials systems and phenomena of interest necessitates the use of model systems and the development of sound theoretical foundations. The ability to 'create' ideal situations in computer-based simulations is one of the great strengths but also one of the most potentially dangerous aspects of *ab initio* calculations because it is presently impossible to fabricate actual experimental specimens with the chemical homogeneity and structural precision that can easily be achieved in simulation. Phenomenological approaches avoid the explicit assumption of perfection by starting from experimental observations, but their extrapolation implicitly assumes a lack of obfuscating circumstances.

The most common assumption that is made when measuring the characteristics of materials of any kind is that the sample is what it is "supposed" to be; in other words, it is assumed that a sample is pure and homogeneous as long as whatever attempts have been made to verify this assumption have not contradicted it. However, often times impurity or other defect concentrations well below the detection limits of whatever techniques were used can still play key roles in the final microstructure, properties, etc. of the sample. The recent separate but equally elegant pieces of work from Dillon and Harmer[2-3] and from Lee *et al.*[4-5] illustrate this point perfectly. Each study revealed new and important modifications to the fundamental understanding associated with processing one of the most extensively studied ceramic systems through careful re-examination with unprecedented precision.

With this in mind, we discuss below the issues associated with size/interface effects of ferroelectric and associated high-permittivity thin films in terms of three separate but related ways in which reality often differs from the ideal (and often assumed) case.

2.1 Phase Effects

Common sense and dielectric mixing rules tell us that the presence of a low-permittivity second phase will result in measured properties inferior to those of the pure high-permittivity phase. This effect is commonly observed in systems that contain one or more volatile cations, such as Pb, Bi, etc.[6-9] It is not necessary, however, that these low-permittivity regions appear as discrete separate phases as observed by diffraction techniques in order to severely degrade properties. This was famously shown, for example, by Frey *et al.* for fine grain $BaTiO_3$ materials.[10] In order to determine the origin of the measured property degradation with decreasing grain size in specimens that were all single-phase according to x-ray diffraction (XRD), Frey and co-workers used complementary techniques combined with dielectric analysis to show that their grain boundaries were acting as a low-permittivity second phase. Fascinating studies from Ihlefeld *et al.* have highlighted a critical difference between grain size as observed by electron microscopy and crystallite size as indicated by diffraction techniques, revealing a better correlation between crystallite size and measured electrical properties than measured grain size and properties.[11] Work from Hoshina and co-workers further emphasized the critical importance of grain and/or crystallite boundaries on electrical performance, showing that grains with sharp interfaces (essentially minimal grain/crystallite boundary volume) exhibited enhanced permittivity when compared to materials containing grains with diffuse changes in lattice parameter.[12]

2.2 Chemical Effects

The work from Wada *et al.* is an excellent example of the blurred interface among chemistry, phase, and interfaces in ceramic dielectrics. While they were able to tweak the lattice parameter distribution in their particles through controlled atmosphere processing and therefore presumably by changing the nature and distribution of ionic defects, no direct evidence of any changes in chemistry was reported. The recent re-examination of the $PbZrO_3$-$PbTiO_3$ phase diagram is another case where cation distribution is likely critical, but because of limitations in the sensitivity and sampling volume of available characterization techniques, homogeneity must be assumed rather than confirmed.[13-16] The relaxor ferroelectrics literature also highlights the role of chemical distribution in observed size effects in ferroelectrics. Extensive studies have shown that the nature and ordering of B-site cation species is directly related to the observed dielectric behavior, and that those differences in cation distribution (associated, for example, with the ordering or clustering of disparate species on the several-unit-cell scale) result in wildly different dielectric behaviors.[17-18]

Achieving equilibrium chemical distributions in ferroelectrics, especially those containing volatile cations, is never as straightforward as simply annealing the materials until entropy drives them to homogeneity. The relatively low diffusion rates of many cations under practical heating conditions combined with varying driving forces associated with chemical reactions mean that the chemical distributions within ferroelectric materials are often as much or more a record of the processing history of the specimen as a representation of equilibrium. This is true whether the samples of interest were grown from a melt, fabricated through solid-state reaction, condensed from a vapor phase, or any number of other possibilities. Again using the PZT system as an example, the work of Calame and Muralt clearly demonstrates this issue.[19] Early work on the PZT system showed that $PbZrO_3$ exhibited a higher Pb vapor pressure and should show a higher crystallization temperature than $PbTiO_3$.[20] Polli and coworkers showed that this is indeed the case for crystallization from the most common solution system for the production of PZT thin films.[21] Earlier efforts had taken advantage of this to promote crystallization via discrete $PbTiO_3$-rich seeds, but it wasn't until Calame and Muralt demonstrated the effects of this preferential $PbTiO_3$-rich nucleation on cation distribution that the level of cation heterogeneity present in such films was really appreciated.[19]

2.3 Interface Effects

The chemical-distribution issues mentioned above all discuss situations associated with materials in which the chemistry of the surroundings should match—or at least be closely related to, as in the case of $PbTiO_3$ seeding—the chemistry of the region of interest. Matters are further complicated when discrete interfaces between dissimilar materials are involved. In addition to chemical distribution and associated reactions, strain, electrostatic, and variable band offset issues can also be present. The experimental work in this arena can largely be separated into two categories: fundamental work on model systems and application-based work that generally involves larger areas and volumes as well as cheaper, more technologically relevant (and typically less ideal) substrates. Theoretical efforts have largely focused on ideal model systems partially because they are selected to minimize the number and magnitude of assumptions required and because they are often operating in size regimes that are more interesting from a fundamental physical phenomena standpoint.

A great deal of excellent work in the past decade has focused on such model systems, and much progress has been made towards understanding the behavior of coherently strained epitaxial ferroelectric thin films.[22-25] Even for these ideal interfaces, however, disagreement exists about the true effects of the interface on the electronic (and thus dielectric and ferroelectric) response. Dozens of papers (see, for example, [26-30]) have been published with theoretical and/or experimental results that support or refute the existence of a paraelectric 'dead layer' at the interfaces between electrodes and a thin ferroelectric.

While focused ion beam (FIB)-cut slices of single crystals and epitaxial films on lattice-matched oxide substrates are great for fundamental studies, such approaches are not feasible for any large-scale application, and ferroelectric films processed by methods which are amenable to such uses come with their own complications. For example, reports vary widely about the properties and potential interactions of films deposited on Pt electrodes.

3. A CASE STUDY: CSD PZT-BASED THIN FILMS

Over the years, the group at Sandia National Laboratories (SNL) has built up significant capabilities and expertise around chemical solution derived (CSD) PZT-based thin films. Here we discuss the chemical, phase, and interface development of such films during processing, and highlight the characterization and analysis tools that we have developed and/or used in this process.

3.1 Fabrication

Fabrication of PZT-based thin films as described here follows the approach originally developed by Yi and Sayer[31] and then modified by Schwartz and Assink.[32] B-site alkoxides (zirconium n-butoxide, titanium isopropoxide and, when desired, niobium n-butoxide) are chelated with glacial acetic acid and then dissolved in methanol. A-site acetates (lead(IV) acetate and, when desired, lanthanum acetate hydrate) are then mixed in and the solution is heated to ~90ºC to dissolve the acetates. Once cool, additional methanol and acetic acid are added to adjust molarity and further stabilize the solution. Using this approach, solutions as concentrated as 0.4M can be stable for years.

These solutions are then spin deposited using a standard photoresist spinner and the resulting samples are dried on a hot plate at temperatures ranging from 100-550ºC. After multiple layers are deposited, the film is crystallized at temperatures ranging from 600-700ºC. The entire solution preparation and deposition process is summarized in Figure 1. Earlier work showed that final film thickness varies linearly with the number of depositions as well as the molarity of the starting solution.[33] Those studies further revealed that the number of deposited layers is much more important for avoidance of pinhole defects and therefore functional device yield than absolute film thickness. For this reason, simply diluting the solution enables the fabrication of ultrathin layers that are electrically functional across macroscopic (mm^2) areas. Other groups have also had success spin coating ultrathin dielectric films from chemical solution.[34-35]

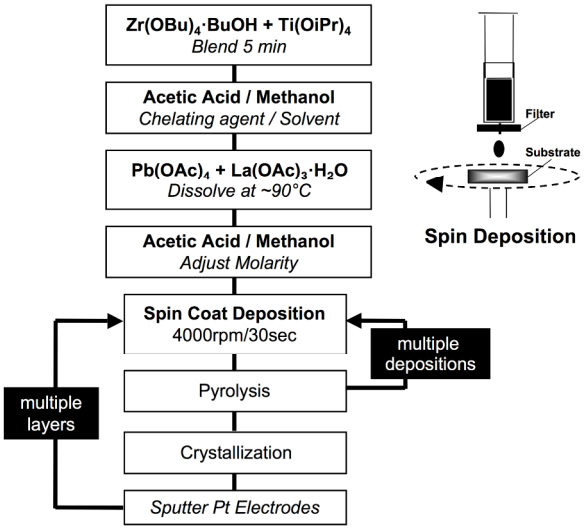

Figure 1 – Schematic illustration of the solution preparation and film deposition process used by SNL for La-modified PZT thin films.

Crystallization of such films can be accompanied by a drive to de-wet the substrate and form islands.[36] Several groups have taken advantage of this for the formation of seed layers that can template subsequent layers for improved film texture and/or reduced crystallization temperatures,[37-40] but such islanding presents a practical limitation to the minimum thickness of crystalline ferroelectric film that can be deposited via CSD. The thinnest continuous PZT film that we have been able to deposit and crystallize on a platinized silicon substrate to date is roughly 9 nm in thickness, as shown in transmission electron microscope (TEM) cross-section in Figure 2.[41]

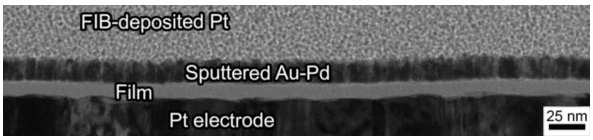

Figure 2 – Cross section image of a 9nm thick CSD PZT film which was continuous and single-phase as determined by X-ray reflectivity and diffraction, as well as by TEM.

The crystallization of Pb-based ferroelectrics into the perovskite phase from solution is not well understood from a fundamental standpoint, but a large number of studies have been carried out which provide empirical descriptions of the process for specific solution chemistries, substrates, and processing conditions. In general, the removal of most or all organic components during pyrolysis results in an amorphous layer that ideally consists of a homogeneous distribution of cations (though several studies have indicated that cation clustering in solution and/or in this amorphous phase is common).[42-44] The conversion of this amorphous layer into the desired homogeneous crystalline perovskite film is a complex process that is influenced by a wide variety of factors, including atomic distribution in the solution/gel state, overall thermal profile, atmosphere, and multiple potential interactions with the substrate, such as chemical diffusion, templating, stress, and several others. Further complicating matters in PZT-based thin films is the fact that—according to multiple studies—crystallization always proceeds by first forming a fluorite-type phase from which the perovskite subsequently grows.[21,43] In instances of sufficient cation ordering, this intermediate phase can actually exhibit the pyrochlore structure, but for simplicity, we will phrase the current discussion in terms of the more general fluorite-type structure.

PZT-based thin films that are deposited on Pt electrodes typically acquire the texture of the underlying electrode, but several groups have shown that varying the thermal profile used for crystallization can result in significantly different texture of the PZT film. One example of this is shown in Figure 3. A single 3" platinized Si substrate was coated with a PZT precursor solution and then diced into multiple pieces. Each piece was then rapidly pyrolized for 1 min at a temperature between 350 and 550°C. All pyrolized pieces were then heated rapidly together at the same time to 700°C for 10 min to crystallize the films, at which point X-ray diffraction was performed. All samples were identified as being single phase perovskite, but the eventual texture of the PZT layer correlated strongly with the initial heat treatment temperature. Figure 3 also demonstrates schematically how the varying pyrolysis treatments might have led to the final film texture. Pyrolysis temperatures less that 420°C likely did not result in the formation of any fluorite crystallites; subsequent perovskite crystallization could then be dominated by heterogeneous nucleation from the underlying <111> Pt electrode. Higher temperature pyrolysis could homogeneously nucleate fluorite crystallites that would lead to perovskite grains independent of the electrode texture. In such cases, large (100) surface rosettes tend to dominate film orientation. Even higher pyrolysis temperatures might lead to widespread nucleation at the electrode surface as well as within the bulk of the film, eventually resulting in mixed film texture.

Temperature and time are both critical factors in the crystallization process; given sufficient time, systems will tend towards their thermodynamically stable form. Reports conflict about the relative thermodynamic stability of the fluorite and perovskite phases in the PZT system under various conditions, but it seems likely that fluorite crystallization is favored by the disorder present during the initial heat treatment steps. This is consistent with *in-situ* diffraction studies that Nittala *et al.* report in their paper at this conference showing a retardation of perovskite formation with excess Pb content. Several groups have attempted to decrease the temperature of perovskite crystallization by increasing the level of cation homogeneity in the gel stage and/or by promoting nucleation through the use of seeds. The most successful of these is the Slovenian group, who managed to achieve perovskite crystallization in Zr-rich films below 500°C.[44-45] Figure 4 gives an example of some low temperature crystallization work on PZT 53/47 films, showing that dielectric constants greater than 1000 can be achieved at temperatures as low as 500°C with extended annealing. Also apparent in Figure 4 is the permittivity decrease after long times at high temperatures due to Pb loss.

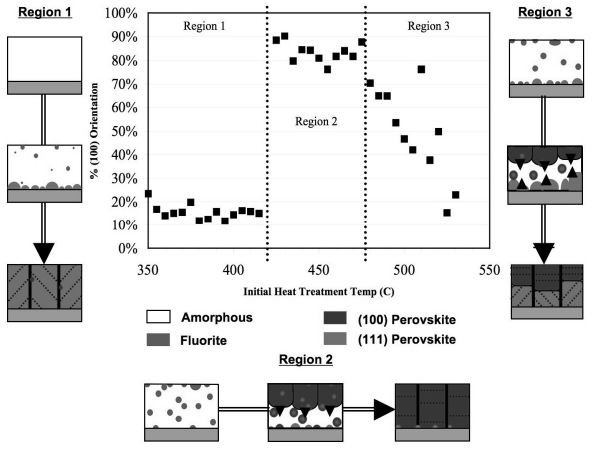

Figure 3 – Effect of pyrolysis temperature on the orientation of PZT 40/60 films after identical crystallization at 700°C and proposed mechanism(s) behind the texture development.

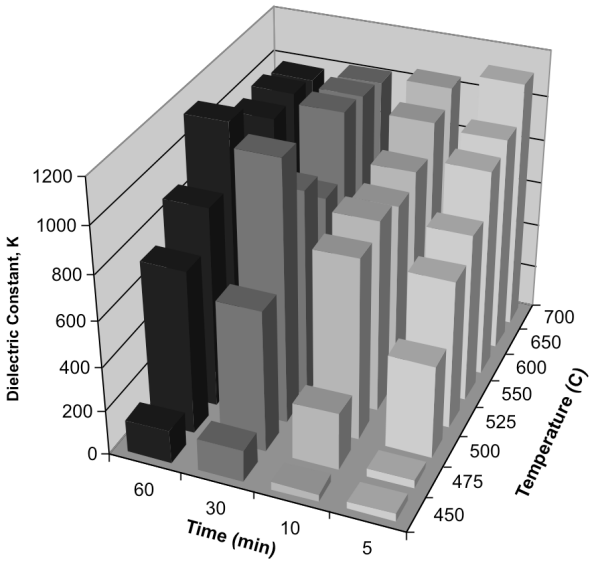

Figure 4 – Measured dielectric constant values of PZT 53/47 films crystallized at temperatures ranging from 450 to 700°C with hold times of 5 to 60 min.

The fluorite structure is able to accommodate significantly greater deviation from stoichiometry than the perovskite structure. Due in part to the volatility of the Pb cation, this fact plays a critical role in the phase formation and distribution in Pb-based ferroelectrics—and likely contributes to the propensity of the fluorite-type phase to crystallize before the perovskite phase. In order to compensate for the inevitable loss of the volatile Pb cation during heat treatment, Pb-based films are typically deposited with excess Pb content, the value of which commonly ranges from ~5-30%. This Pb excess promotes further interactions between the Pb in the film and Pt substrates that not only provides another mechanism for Pb depletion from the film, but also degrades the electrical conductivity of the Pt electrode. More importantly, though, Pb diffusion through the Pt electrode to the TiO_2/SiO_2 adhesion layers can lead to reactions that result in de-adhesion from the Si substrate and film peeling. Since the perovskite phase is much less tolerant of non-stoichiometry than the fluorite-type phase(s), lead loss occurs less quickly from the perovskite phase(s) than from the fluorite—this principle applies whether the loss is through volatilization in the vapor phase or diffusion into the bottom electrode.

One approach that our group developed in an attempt to minimize deleterious interactions with the electrode is to intentionally fabricate Pb-deficient films in direct contact with the bottom Pt electrode. Rather than fighting a losing battle of trying to balance Pb loss with Pb excess, starving the films of Pb in the first place minimizes the interactions between the film and the electrode. Thanks to the tendency of perovskite PZT films to preferentially nucleate at the Pt electrode surface, the microstructure that results consists essentially of a nearly-stoichiometric protective (i.e., lower-Pb diffusivity) perovskite layer covered with a Pb-deficient fluorite layer. As reported previously, a post-crystallization annealing step in the presence of significant Pb excess (most easily achieved by spinning a PbO solution atop the sample) can then convert the sample to fully single-phase perovskite with excellent ferroelectric properties.[46] This approach does not entirely eliminate but does reduce Pb diffusion into the underlying Pt electrode.

The source of excess Pb used to drive conversion of the already-crystallized film into single-phase perovskite is not critical. Instead of a PbO solution, for example, a Pb-rich PZT-based solution can be used to both supply the underlying mixed-phase layer with sufficient Pb for conversion to perovskite and to deposit an additional stoichiometric PZT layer. Figure 5 demonstrates this by showing the dielectric properties of ~50nm thick PLZT 12/70/30 films that were initially formed from nominally stoichiometric solutions and therefore contained substantial Pb-deficient fluorite after crystallization. Depositing a PbO layer immediately after pyrolyzing the PLZT layers and then crystallizing the films at 700°C for 10 min improves the dielectric constant somewhat, as shown to the far left. Annealing the samples at 300°C after sputter deposition of the top Pt electrodes produced insignificant changes in measured properties, but depositing a Pb-rich layer (a solution of either PbO or the same PLZT 12/70/30 composition but with 20% excess Pb) and then heating to 700°C to crystallize this layer resulted in dramatic improvements in the properties of the underlying PLZT

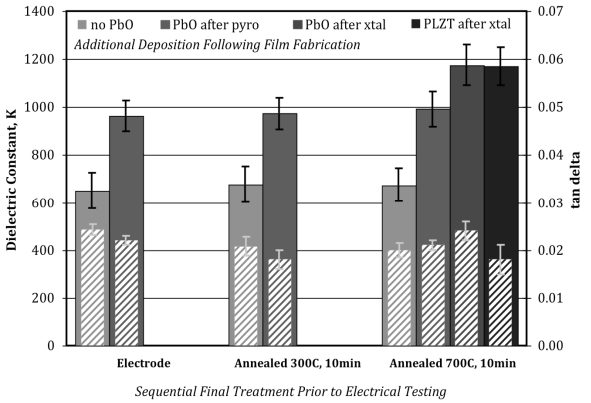

Figure 5 – PLZT 12/70/30 films fabricated from nominally stoichiometric solutions show poor dielectric properties immediately after crystallization and after 300°C annealing of the sputtered top electrode, even when coated with PbO between pyrolysis and crystallization. Crystallizing a Pb-rich layer on top of these electroded samples greatly improved the dielectric properties of the original bottom layer by converting Pb-deficient fluorite to perovskite.

layer which had been previously crystallized. Interestingly, while the Pb-deficient crystallization approach was developed in large part to counteract problems arising from Pb diffusion into and through Pt, this rapid diffusion actually turns out to be convenient when fabricating multilayer structures. Internal Pt electrodes are deposited directly on the PZT-based dielectric layers with no need for an adhesion layer, so other than a relatively small decrease in the Pt conductivity, there are no problems associated with Pb diffusion into these electrodes, and they provide essentially no barrier to Pb diffusion between a Pb-deficient fluorite layer and an overlying Pb-rich gel.

The pinhole-free nature of these films enables the fabrication of functional capacitors with enormous area/thickness aspect ratios and thus very large capacitance values. However, for many applications, substrate real estate is at a premium, so increasing the effective area without increasing the capacitor footprint is advantageous. Towards this goal, we built upon the earlier work from others[47-50] and fabricated functional, parallel-connected multilayer capacitor structures based upon alternate layers of solution-deposited dielectric layers and sputtered electrode layers. Performing multiple crystallization steps in this manner with a Pb-rich solution initially deposited on the bottom Pt electrode results in delamination from the Si substrate due to Pb reaction with the TiO_2/SiO_2 adhesion layers after diffusion through the base Pt electrode. By depositing a Pb-deficient bottom layer and then relying upon Pb diffusion through subsequent buried Pt electrodes, we were able to fabricate structures in which each PZT-based layer was single-phase perovskite without the delamination that would normally result from cycling through multiple crystallization steps, as shown in Figure 6.

3.2 Electrode-Film Interface

The electrical performance of these ultrathin multilayer capacitor (UTMLC) structures has been reported previously,[51] and shows that while the dielectric layers are

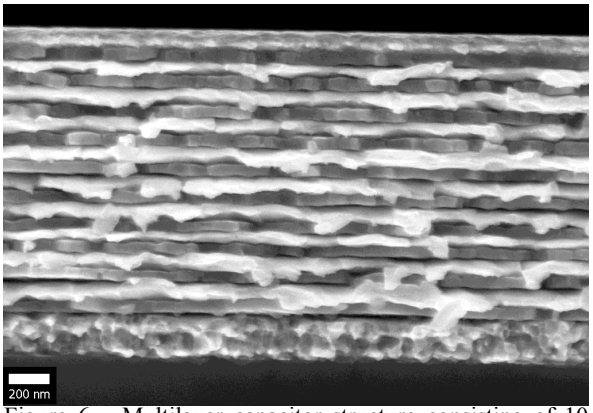

Figure 6 – Multilayer capacitor structure consisting of 10 PZT layers ~50nm thick alternating with sputter-deposited Pt inner electrodes all on top of a $Pt/TiO_2/SiO_2/Si$ substrate.

all single phase as determined by X-ray diffraction and TEM, there is still a significant degradation in properties for film properties for layer thicknesses less than ~50nm. While the Pb-deficient approach allows us to fabricate functional structures without delamination, the ideal situation would be to use electrode layers that do not interact with the PZT-based dielectric layers chemically. For applications such as high speed integrating capacitors or pulse discharge capacitors, however, the resistance of the electrodes must remain sufficiently low as not to impede rapid charge transport. For this reason, oxide electrodes such as $LaNiO_3$ or $SrRuO_3$ are not good options. Our initial work with Ir electrodes indicated significantly greater interaction between the Ir and the PZT-based layer than seen with Pt (see Figure 7), so it was determined that sputtered Ir electrodes were not feasible for use with CSD PZT-based capacitors.

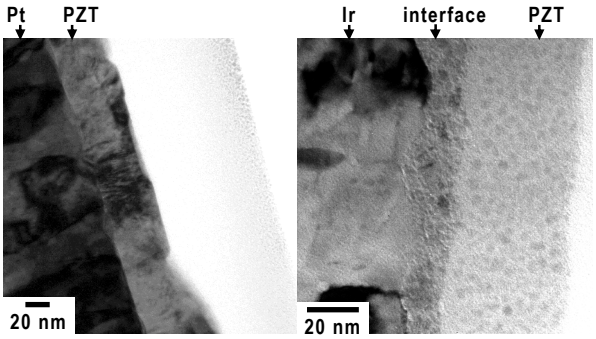

Figure 7 – TEM cross sections comparing the electrode-PZT interface for films deposited on Pt (left) and Ir (right). Pt electrodes show a relatively clean interface with the PZT layer, but significant interaction is seen with the Ir electrode.

Another potential electrode material under investigation is ZrB_2, sputter deposited using a target fabricated by hot pressing at Missouri University of Science and Technology. As deposited, the ZrB_2 thin films were dense, fine grain and nearly as conductive as sputtered Pt films. XPS studies showed that the first one to two atomic layers were oxidized, but that the bulk of the film contained mostly ZrB_2 with a relatively small amount of ZrO_2, as the bond energy spectra were dominated by Zr-B bonds (Figure 8). After solution deposition of PZT-based thin films, a slightly thicker

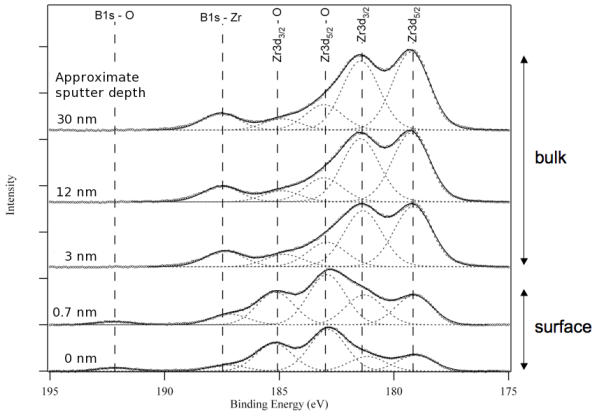

Figure 8 – XPS data of the binding energies measured for Zr and B species in a sputtered ZrB_2 thin film showing that B-O bonds are present on the very surface of the film, and that the bulk film contains some ZrO_2 but is dominated by ZrB_2.

interfacial layer developed, as seen in the TEM cross-section image in Figure 9. Boron X-rays are very soft and are therefore difficult to map by energy dispersive spectroscopy (EDS); high-z elements such as Zr are not very amenable to electron energy loss spectroscopy (EELS), so quantifying the chemistry of this interface layer in the TEM is very challenging. Figure 10 shows a composite image created from a series of energy filtered TEM (EFTEM) images. While not conclusive, these results combined with further XPS data indicate further oxidation of the ZrB_2 surface, but little if any additional interactions with the PZT layer.

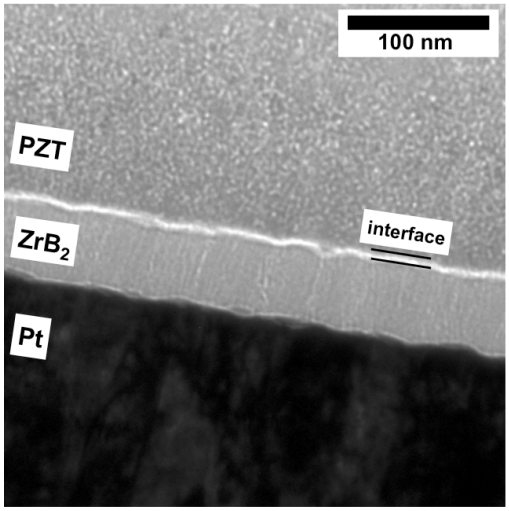

Figure 9 – TEM cross section showing a thin but discrete interface between ZrB2 and PZT that has a lower average atomic number than either of the films themselves.

3.3 Cation Diffusion and Heterogeneity

One of the greatest difficulties in the fabrication of complex oxide thin films has always been achieving quantitative chemical analysis on the size scales commensurate with the feature size(s) of interest. For example, SIMS and XPS offer high sensitivity and high depth resolution, but attain signal from tens of square microns of surface area. Standard EDS linescans across

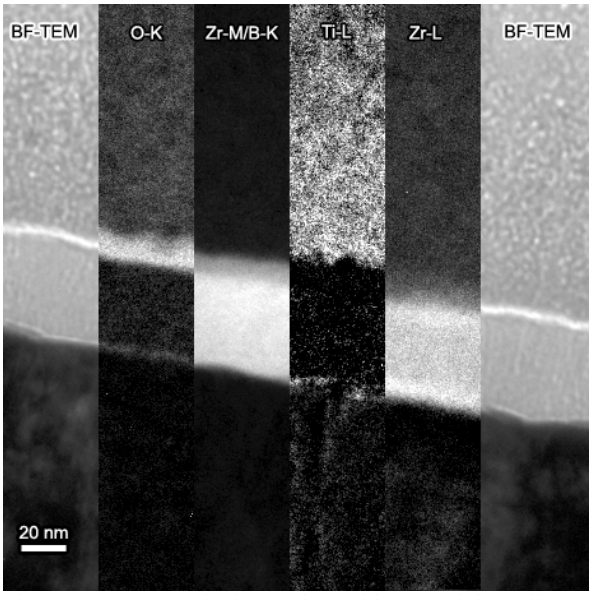

Figure 10 – Composite image formed by combining adjacent sections of EFTEM images of the same film shown in Figure 9, indicating oxidation of the ZrB_2.

the thickness of a film cross section provide information of appropriate length scales along the direction of the scan, but less than 10nm normal to the scan direction. By acquiring EDS maps and then combining multivariate statistical and principle component analyses (MVSA and PCA), we are able to collect standard-based quantitative chemical information across the entire sample region of interest with single-pixel lateral resolution. Details of this work are published elsewhere,[52-53] but Figure 11 shows some of what these techniques make possible. From the top two images, we can see the distinct differences between Pb-deficient fluorite (orange) and stoichiometric perovskite (yellow) phases in a mixed-phase sample prepared from a Pb-deficient solution, and then the homogeneous Pb distribution in an identical sample that was then coated with PbO and heated again. From the same data sets, it is possible to pull out the cation distributions with sufficient resolution to see the Zr segregation that occurs as the perovskite phase preferentially grows Ti-rich and essentially pushes the Zr into the fluorite region ahead of the perovskite growth front. Further, there is slight but significant segregation of La that closely mirrors the Zr distribution, indicating the possibility of co-segregation, potentially in the form of a $La_2Zr_2O_7$ phase, which has been observed in bulk PLZT materials.[54]

4. SUMMARY

PZT-based thin films are useful for a wide range of different applications, and CSD offers an inexpensive and effective fabrication approach. Property optimization on technologically relevant substrates and electrodes, however, requires a more complete understanding of the phase and interface development of these systems. Capturing such a complete picture requires the amalgamation of information from a variety of complementary characterization techniques across a broad spectrum of experimental parameter space, which can then drive further advances in fabrication.

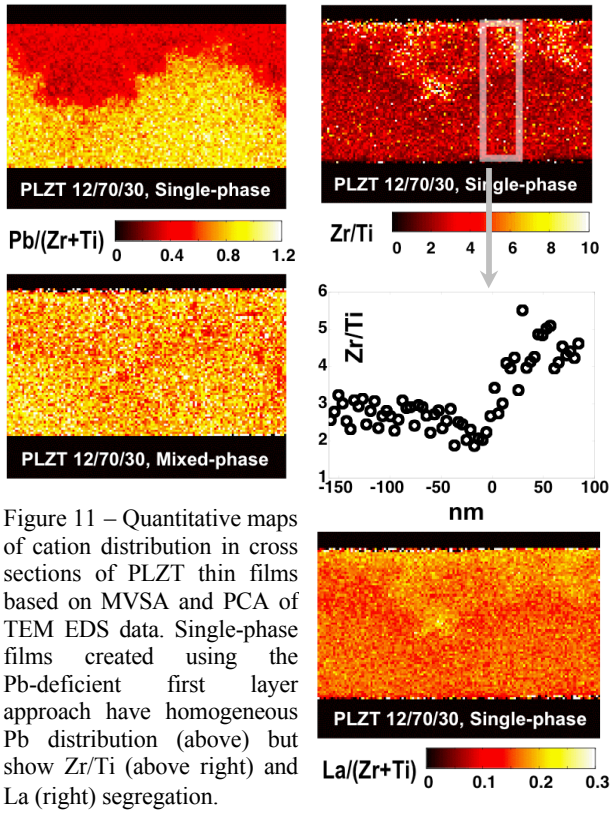

Figure 11 – Quantitative maps of cation distribution in cross sections of PLZT thin films based on MVSA and PCA of TEM EDS data. Single-phase films created using the Pb-deficient first layer approach have homogeneous Pb distribution (above) but show Zr/Ti (above right) and La (right) segregation.

5. ACKNOWLEDGEMENTS

The authors gratefully acknowledge the technical assistance of P. A. Mahoney, D. L. Moore, L. N. Brewer, M. J. Rye and J. F. Ihlefeld of Sandia National Laboratories, J. Sigman of Micron Technologies, A. Sehirlioglu of Case Western Reserve University and NASA Glenn Research Center, and D. M. Marincel, W. G. Fahrenholtz, and H. J. Brown-Shaklee of Missouri University of Science and Technology. Sandia is a multiprogram laboratory operated by Sandia Corporation, a Lockheed Martin Company, for the United States Department of Energy's National Nuclear Security Administration under contract DE-AC04-94AL85000.

6. REFERENCES

[1] V. L. Ginzburg, *Zh. Eksp. Teor. Fiz.* **15** 739 (1945); *J. Phys USSR*, **10** 107 (1946).
[2] S. J. Dillon and M. P. Harmer, *J. Am. Ceram. Soc.*, **91**, 2304-13 (2008).
[3] S. J. Dillon and M. P. Harmer, *J. Am. Ceram. Soc.*, **91**, 2313-20 (2008).
[4] S. Lee, C. A. Randall and Z.-K. Liu, *J. Am. Ceram. Soc.*, **91**, 1748-52 (2008).
[5] S. Lee, C. A. Randall and Z.-K. Liu, *J. Am. Ceram. Soc.*, **91**, 1753-61 (2008).
[6] K. H. Hardtl and H. Rau, *Solid State Comm.*, **7**, 41-5 (1969).
[7] G. S. Snow, *J. Am. Ceram. Soc.*, **56**, 479-80 (1973).
[8] K. H. Hardtl and D. Hennings, *J. Am. Ceram. Soc.*, **55**, 230-1 (1972).

[9] S.-E. Park, S. J. Chung, I. T. Kim and K. S. Hong, *J. Am. Ceram. Soc.*, **77** 2641-7 (1994).
[10] M. H. Frey, Z. Xu, P. Han, and D. A. Payne, *Ferroelectrics*, **206-207**, 337-53 (1998).
[11] J. F. Ihlefeld, A. M. Vodnick, S. P. Baker, W. J. Borland and J. P. Maria, *J. Appl. Phys.*, **103**, 074112 (2008).
[12] T. Hoshina, S. Wada, Y. Kuroiwa and T. Tsurumi, *Appl. Phys. Lett.*, **93**, 192914 (1998).
[13] B. Noheda, J. A. Gonzalo, L. E. Cross, R. Guo, S.-E. Park, D. E. Cox and G. Shirane, *Phys. Rev. B*, **61**, 8687-95 (2000).
[14] A. M. Glazer, P. A. Thomas, K. Z. Baba-Kishi, G. K. H. Pang and C. W. Tai, *Phys. Rev. B*, **70**, 184123 (2004).
[15] M. Budimir, D. Damjanovic and N. Setter, *Phys. Rev. B*, **73**, 174106 (2006).
[16] K. A. Schonau, L. A. Schmitt, M. Knapp, H. Fuess, R.-A. Eichel, H. Kungl and M. J. Hoffmann, *Phys. Rev. B.*, **75**, 184117 (2007).
[17] L. Farber and P. K. Davies, *J. Am. Ceram. Soc.*, **86**, 1861-6 (2003).
[18] G. A. Samara, *Phys. Rev. B*, **71**, 224108 (2005).
[19] F. Calame and P. Muralt, *Appl. Phys. Lett.*, **90**, 062907 (2007).
[20] A. P. Wilkinson, J. S. Speck, A. K. Cheetham, S. Natarajan and J. M. Thomas, *Chem. Mater.*, **6**, 750-4 (1994).
[21] A. D. Polli, F. F. Lange and C. G. Levi, *J. Am. Ceram. Soc.*, **83**, 873-81 (2000).
[22] D. D. Fong and C. Thompson, *Annu. Rev. Mater. Res.*, **36**, 431-65 (2006).
[23] K. J. Choi, M. Biegalski, Y. L. Li, A. Sharan, J. Schubert, R. Uecker, P. Reiche, Y. B. Chen, X. Q. Pan, V. Gopalan, L.-Q. Chen, D. G. Schlom and C. B. Eom, *Science*, **306**, 1005-9 (2004).
[24] M. Stengel and N. A. Spaldin, *Nature*, **443**, 679-82 (2006)
[25] M. Stengel, D. Vanderbilt and N. A. Spaldin, *Nat. Mater.*, **8**, 392-7 (2009).
[26] L. W. Chang, M. McMillen, F. D. Morrison, J. F. Scott and J. M. Gregg, *Appl. Phys. Lett.*, **93**, 132904 (2008).
[27] T. M. Shaw, S. Trolier-McKinstry and P. C. McIntyre, *Annu. Rev. Mater. Sci.*, **30**, 263-98 (2000).
[28] V. Petkov, V. Buscaglia, M. T. Buscaglia, Z. Zhao and Y. Ren, *Phys. Rev. B*, **78**, 054107 (2008).
[29] M. Dawber, K. M. Rabe and J. F. Scott, *Rev. Mod. Phys.*, **77**, 1083-1130 (2005).
[30] U. Ellerkmann, T. Schneller, C. Nauenheim, U. Bottger and R. Waser, *Thin Solid Films*, **516**, 4713-9 (2008).
[31] G. Yi, Z. Wu and M. Sayer, *J. Appl. Phys.*, **64**, 2717-24 (1988).
[32] R. A. Assink and R. W. Schwartz, *Chem. Mater.*, **5**, 511-7 (1993).
[33] G. L. Brennecka and B. A. Tuttle, *J. Mater. Res.*, **22**, 2868-74 (2007).
[34] A. Hardy, S. V. Elshocht, J. D'Haen, O. Douheret, S. De Gendt, C. Adelmann, M. Caymax, T. Conrad, T. Witters, H. Bender, O. Richard, M. Heyns, M. D'Olieslaeger, M. K. Van Bael, J. Mullens, *J. Mater. Res.*, **22**, 3484-93 (2007).
[35] J. Ricote, S. Holgado, Z. Huang, P. Ramos, R. Fernandez and M. L. Calzada, *J. Mater. Res.*, **23**, 2787-95 (2008).
[36] K. T. Miller, F. F. Lange and D. B. Marshall, *J. Mater. Res.*, **5**, 151-60 (1990).
[37] S. Hiboux and P. Muralt, *J. Euro. Ceram. Soc.*, **24**, 1593-6 (2004).
[38] S. Buhlmann, P. Muralt and S. Von Allmen, *Appl. Phys. Lett.*, **84**, 2614-6 (2004).
[39] A. Wu, P. M. Vilarinho, I. Reaney and I. M. Miranda Salvado, *Chem. Mater.*, **15**, 1147-55 (2003).
[40] R. W. Schwartz, J. A. Voigt, B. A. Tuttle, D. A. Payne, T. L. Reichert and R. S. DeSalla, *J. Mater. Res.*, **12**, 444-56 (1997).
[41] J. Sigman, G. L. Brennecka, P. G. Clem and B. A. Tuttle, *J. Am. Ceram. Soc.*, **91**, 1851-5 (2008).
[42] A. D. Polli and F. F. Lange, *J. Am. Ceram. Soc.*, **78**, 3401-4 (1995).
[43] B. A. Tuttle, T. J. Headley, B. C. Bunker, R. W. Schwartz, T. Zender, C. L. Hernandez, D. C. Goodnow, R. J. Tissot, J. Michael and A. H. Carim, *J. Mater. Res.*, **7**, 1876-82 (1992).
[44] B. Malic, I. Arcon, A. Kodre and M. Kosec, *J. Appl. Phys.*, **100**, 051612 (2006).
[45] M. Mandeljic, B. Malic, M. Kosec and G. Drazic, *Integ. Ferro.*, **46**, 329-38 (2002).
[46] G. L. Brennecka, C. M. Parish, B. A. Tuttle, L. N. Brewer and M. A. Rodriguez, *Adv. Mater.*, **20**, 1407-11 (2008).
[47] Y. Sakabe, Y. Takeshima and K. Tanaka, *J. Electroceram.*, **3**, 115-21 (1999).
[48] M. Grossman, R. Slowak, S. Ho□mann, H. John and R. Waser, *J. Euro. Ceram. Soc.*, **19**, 1413-15 (1999).
[49] S. Wang, A. Kawase and H. Ogawa, *Jpn. J. Appl. Phys.*, **45[9B]**, 7353-58 (2006).
[50] M.M. Watt, *Integrated Ferroelectrics*, **26**, 163 (1999).
[51] G. L. Brennecka, C. M. Parish, B. A. Tuttle and L. N. Brewer, *J. Mater. Res.*, **23**, 176-81 (2008).
[52] C. M. Parish, G. L. Brennecka, B. A. Tuttle and L. N. Brewer, *J. Am. Ceram. Soc.*, **91**, 3690-7 (2008).
[53] C. M. Parish and L. N. Brewer, *submitted to Ultramicroscopy* (2009).
[54] C. M. Parish and B. A. Tuttle, unpublished (2008).